

Activation of mass transfer processes at spark plasma sintering of zirconium dioxide

S A Akarachkin¹, A S Ivashutenko² and N V Martyushev²

¹ 'SIC 'Polus' JSC, 56B, Kirova ave., Tomsk, 634050, Russia

² National Research Tomsk Polytechnic University, 30, Lenina ave., Tomsk, 634050, Russia

E-mail: ivashutenko@tpu.ru

Abstract. The paper presents the results of numerical simulation of thermal and electric fields' distribution in the graphite moulding tool and in the sintered sample of $ZrO_2-4\%Y_2O_3$ in the course of spark plasma sintering (SPS). The reduction of SPS duration is accounted for the largeness of specific thermal flux towards the sample surface, emitted by the graphite moulding tool. The impact of the electric field on the sample structure leads to emergence of the polarizing processes forcing zirconium ions to shift from lattice sites, which is able to reduce the required value of thermal energy necessary for initiation of a diffusion process. The axial pressure at high temperatures of sintering can lead to plastic deformation of the powder particles.

1. Introduction

Engineering ceramics has found its wide application in many branches of industry such as nuclear, chemical, aerospace and in a number of others. The manufacturing procedure of engineering ceramics has been constantly improved towards reduction of expenditures for production unit manufacturing. Of no small importance task is enhancement of service properties of production in order to increase its service life period.

For solution of the set tasks a multiple of technological solutions has been developed. For the purpose of obtaining ceramics with a fine-grained structure the nanopowders with subsequent methods of high-energy influence are applied, for example, impulse pressing [1-3], sintering in glow-discharge plasma [4], sintering in the electric microwave field [5] or in charge-particle beam [6].

One of the traditional methods of activated sintering, which reduces the time of heat-treatment, is hot pressing [7]. The reduction of the sintering time allows decelerating the recrystallization process, which enables obtaining a more refined structure and, consequently, enhanced service properties.

A hot-pressing method has obtained further development. In the literature there are several different names of the new method: sintering assisted by electric field (FAST), sintering activated by electric current (ECAS), sintering by pulse current (PECS) [7-9]. However, the producers of the manufacturing equipment promote a market name of the technology, which is 'Sparkle plasma sintering' (SPS) [7].

Sparkle plasma sintering (SPS) is a method of densification of a porous body with the use of the external pressure as well as thermal and electric fields. There are several theories about the mass transfer mechanism at SPS: plastic deformation, electroplastic deformation, electromigration, local temperature gradient at points of sparkle discharge between particles [8, 10].



Depending on the ratio of electric conductivity of the sintered material and the material of the mould, different of the above-mentioned phenomena can reveal themselves.

The method of hot pressing and SPS are quite similar. In both cases the mould with punches are used. However, SPS and hot pressing have a significant difference in the heating mode. In the installations of hot pressing the array of heating elements is used, which heats punches and matrix (hereafter referred to as 'pressing-tool') as well as the sintered material with heat radiation, convection and/or due to heat conductivity of the latter. In case of SPS the electric charge and Joule heat are directly transferred to the sintered material. As far as electric current, passing through a graphite pressing-tool, can reach high density, the heating rate of the material can reach 10^6 °C /s. The heating rate at hot pressing is much lower and amounts to about 80 °C/min [7].

Many, especially earlier studies, explained the SPS efficiency by creation of discharge arc between the powder particles or plasma formation around particles [7].

In early methods PS plasma could actually form due to applied high voltage to a sample, but in modern installations with conducting graphite matrices and low operating voltage, plasma formation is unlikely [7].

Active studies with application of atomic emission electroscopy, direct observation and high-speed voltage measurement did not reveal plasma presence at SPS. Due to the fact that the heating of the pressing-tool and the sintered material at SPS is a consequence of electric current flow, it becomes quite difficult to differentiate the effects caused by high temperature, current and voltage effects. There were assumptions that the applied electric field increases mobility and concentration of defects in the grain boundary structure and influences diffusion assisted energy. However, it has been shown that electromigration is not a dominating mechanism of diffusion. Theoretical calculations have shown that electromigration can exert significant influence only in the systems with low porosity or in ultrafine powders.

Earlier the authors demonstrated the possibility of sintering of zirconium dioxide powder due to formation of local temperature gradients in the area of sparkle discharges between the particles. SPS methodology assumed the use of high-tension pulse voltage source.

2. Materials and methods

At present the installations for SPS, using conducting graphite matrices and pulsed direct current sources, have gained the widest spread [7]. Therefore, the authors set an urgent task to study the processes occurring at ceramic powders sintering at this kind of installations.

In the experiments on sintering stabilized zirconium dioxide containing 96 mas. % ZrO_2 + 4 mas. % Y_2O_3 the SPS installation of 'HP D 10' brand produced by FCT Systeme GmbH Company was used. In fig. 1 the general view of the pressing-tool is shown. The powder was poured into a graphite matrix (3) with inner diameter of 20 mm. Inner surface of the matrix and butt ends of the punches (4, 5) contacting the powder (6), were preliminary protected by the graphite foil of 0.2 mm thick. Then the pressing-tool was located in the vacuum water-cooled chamber and fixed by pushers (1, 2) connected to pulse current source. The following sintering process parameters were set: the rate of temperature rise (200 °C/min), soaking time at sintering temperature (10 min.), and cooling rate, in addition the values of the residual pressure in the vacuum chamber (10 Pa) as well as the power of influence of pushers on punches of the graphite matrix (32 MPa) were indicated. After exhaustion of the water-cooled chamber the force was applied to pushers, then the pulse current generator started its operation. The duration of the rectangular current pulse was 25 ms, after which there was a 5 ms pause.

3. Results and discussion

To calculate the parameters of the thermal condition of SPS let us use the basic Fourier conduction law [9]. Since the pressing-tool (Figure 1) has an axially-symmetric shape, the heat-conducting equation can be written as follows:

$$cC_p \frac{\partial T}{\partial t} = \frac{1}{r} \frac{\partial}{\partial r} \left(r \lambda_r \frac{\partial T}{\partial r} \right) + \frac{\partial}{\partial z} \left(\lambda_z \frac{\partial T}{\partial z} \right) + \dot{q}_i \quad (1)$$

where, γ , C_p , λ_r , λ_z , T , t are density, specific heat, heat conductivity factor along axes r and z , temperature and time correspondingly; \dot{q}_i represents the quantity of heat generated by the inner sources of the system in a unit of volume per a time unit.

Distribution of electric current is described by Kirchhoff equation [9].

$$\frac{1}{r} \frac{\partial (r i_r)}{\partial r} + \frac{\partial (i_z)}{\partial z} = 0 \quad (2)$$

where i_r and i_z are the current density along axes r and z .

Specific power of heat release \dot{q}_i is connected with current density by Ohm's law [9].

$$\dot{q}_i = i_r \rho_r + i_z \rho_z \quad (3)$$

where ρ_r and ρ_z are electric resistance along axes r and z .

When sintering by SPS method Joule heat \dot{q}_i is generated in all components of the system through which the electric current flows. The heat transfer between the parts of the system occurs mainly due to heat conductivity. The heat losses occur because of heat radiation from the graphite pressing-tool as well as heat conductivity from the pusher surfaces coming in contact with water-cooled electrodes.

Stefan-Boltzmann law describes heat transfer at heat radiation.

$$\dot{q}_r = \sigma_s \varepsilon (T_e^4 - T_a^4) \quad (4)$$

where σ_s – Stefan-Boltzmann constant, T_e – temperature of the radiating surface, T_a – temperature of the absorbing surface or environment (300 K [8, 9]), ε – relative emissivity (0.8 [8, 9]), \dot{q}_r - specific power of heat loss by radiation per a time unit from the surface unit.

Heat transfer from the pressing-tool to the water-cooled electrodes is determined as a convective cooling and is described by the following expression:

$$\dot{q}_{conv} = h(T_p - T_w) \quad (5)$$

where T_p , T_w and h – temperatures of the pushers located next to the electrodes, temperature of cooling water (300 K [8, 9]) and a coefficient of the convective heat exchange (880 W/(m \cdot °C) [8, 9]).

Modelling of the heating process was realised along with the replacement of pulse current by direct one. An essential condition of the replacement was the unity of the emitted quantity of heat in the pressing-tool and in the sintered sample per time unit. Thus the connection of the magnitude of pulse current with the equivalent value of the direct current can be described by the following expression:

$$I_C = I_P \sqrt{\tau_H / T_H} \quad (6)$$

where I_C – direct current magnitude, I_P – peak pulse current, τ_H – pulse duration, T_H – pulse repetition period.

The magnitudes of peak pulse voltage U_P and equivalent direct one U_C are related in a similar way.

The solution of the system of equations (1) - (5) in a specified geometric area (see fig. 1) was carried out in COMSOL software package. The operation of this programme is based on numerical solution of a set of differential equations in partial derivatives by the method of finite elements. Before modelling the electrical and thermal characteristics of the following materials were determined: 4Y-ZrO₂, graphite and graphite foil [8, 9].

In a computational model a porous powder body, which represents an initial sample at the beginning of sintering, has been replaced by ceramics of the corresponding composition. A similar approach has shown an excellent accuracy of temperature measurement of all the elements of the pressing-tool and the sintered sample in SPS process [8, 10].

The basic results of modelling are shown in table 1, where I_p and U_p – peak current and peak voltage of power supply, P – total amount of generated energy in volume of the pressing-tool and the sintered sample, P_s – specific heat energy, transferred from the pressing-tool to the sintered sample, T_{Smax} and T_{Smin} – maximum and minimum temperatures in the volume of the sintered sample, Q_s – specific electric charge accumulated by the sintered sample per time of one pulse, ΔU_s – electric voltage drop on the sintered sample.

Table 1 – The results of heat and electric calculations of the experimental model.

I_p , A	U_p , V	P , W	P_s , W/cm ³	T_{Smax} , °C	T_{Smin} , °C	Q_s , C/cm ³	ΔU_s , V
600.00	3.83	1911.60	2.02	734.47	729.52	$8.12 \cdot 10^{-9}$	0.86
648.33	4.11	2219.80	3.28	823.68	819.05	$1.40 \cdot 10^{-8}$	0.93
696.67	4.40	2554.00	4.85	910.78	904.66	$1.55 \cdot 10^{-8}$	1.01
745.00	4.70	2916.30	6.73	995.37	987.08	$1.71 \cdot 10^{-8}$	1.08
793.33	5.01	3309.30	8.90	1077.60	1066.60	$1.66 \cdot 10^{-8}$	1.16
841.67	5.33	3736.10	11.36	1157.80	1143.30	$1.37 \cdot 10^{-8}$	1.24
890.00	5.67	4200.40	14.07	1237.20	1217.70	$1.27 \cdot 10^{-8}$	1.32
938.33	6.02	4706.80	17.04	1315.40	1290.00	$1.36 \cdot 10^{-8}$	1.41
986.67	6.40	5264.40	20.26	1392.70	1360.70	$1.71 \cdot 10^{-8}$	1.50
1035.00	6.81	5871.80	23.61	1469.40	1430.30	$1.93 \cdot 10^{-8}$	1.59

When using SPS method a graphite pressing-tool, through which pulse current flows predominantly, is used for sintering dielectric powders by the primary source of Joule heat. The stabilised zirconium dioxide at temperatures of about 800 °C and higher possesses high ionic conductivity, that is becomes a solid electrolyte [10, 12]. The presence of vacancies in the anionic sublattice of the stabilised zirconium dioxide leads to oxygen transfer according to a vacancy mechanism. Under the influence of pulse electric field there is an oxygen ion drift in the direction of anode in the sample. This is the way the mass transfer process can be activated. Besides the growth of ionic conductivity the stabilised zirconium dioxide acquires abnormal high values of dielectric permittivity $\sim 1 \cdot 10^6$ at heating. Electric charge stored in the sample volume can also influence the mobility of ions in the lattice sites.

In paper [13-16] on SPS the composition α -Al_{2-2x}Fe_{2x}O₃ ($x = 0.02, 0.05, 0.07, 0.10$) was used. Sintering was carried out at temperature of 1350-1450 °C. The samples had a pill-shaped form with the diameter of 8 mm and the height of 2 mm. The voltage on the pressing-tool amounted to 10-20 V.

In the surface layers of samples of 30-40 μ m thickness a composite consisting of α -Fe and α -Al₂O₃ particles was found. It is noteworthy that in the cathode fall region the composite was separated from the sample bulk by the layer with the scanty content of Fe particles. At sintering temperature Fe³⁺ ions were transferred towards the cathode under influence of electric field.

On the basis of data from table 1 it is possible to suggest the predominance of thermal diffusion flows over the ion flows conditioned by the electric field influence. Per time unit the amount of specific heat energy obtained by the sample reaches ~ 24 J/cm³. Specific energy of the electric field accumulated in the sample does not exceed $\sim 1 \cdot 10^{-7}$ J/cm³. Maximum value of electric field intensity in the sample volume is less than 0.3 V/mm. At such low electric field energy it is unlikely that polarized processes, capable of initiating the zirconium ion drift through the existing vacancies in sample lattice structure, will develop.

To evaluate the pattern of electric current distribution between the sample and the pressing-tool let us consider Figure 1. Hereinafter all graphs are presented for the case of usage of amplitude of pulse current $I_p = 1035$ A, see table 1.

Owing to a significant difference in specific electric conductivity electric current flows preliminary along the graphite pressing-tool. Maximum current density and correspondingly the greatest amount of

the generated heat energy fall at graphite punches. Active heat irradiation takes place from the matrix surface by emission, which leads to formation of the temperature gradient between the sample centre and its peripheral area adjacent to the matrix. The magnitude of this gradient increases nonlinearly in accordance with expression (4) at the temperature increase of the pressing-tool, see table 1.

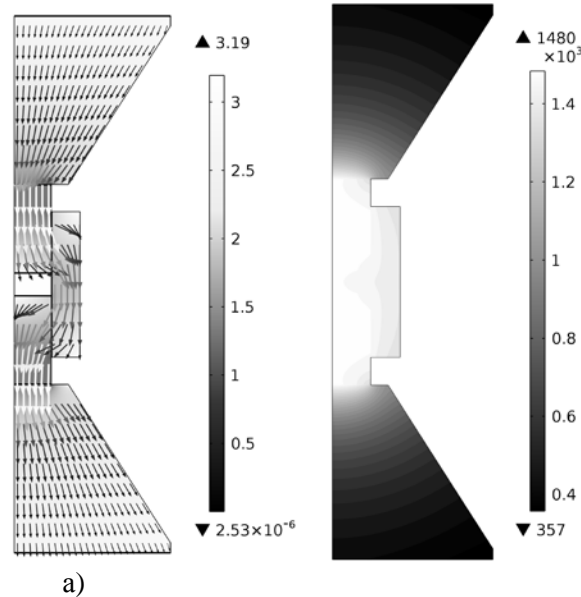


Figure 1. a) current density distribution in the experimental model, arrows show the direction of current flow; the arrow length and colour show the magnitude, in A/mm^2 ; b) temperature field in the experimental model, in $^{\circ}C$.

As the installation for SPS uses pulse current source, the process of charging the geometric capacitance at sintering of dielectric materials takes place, which can influence the law of voltage variation on the sintered sample.

For the analysis of this process let us use a simplified calculation model representing a ring segment of the matrix with a sample located inside of it. The height of the matrix segment and that of the sample is equal. The dielectric material of the sample is replaced by the parallel connected capacitor and resistor. The calculation was conducted in MATLAB/Simulink mathematical software package. The values of the numerical values used in the model were specified according to the results of modeling in COMSOL.

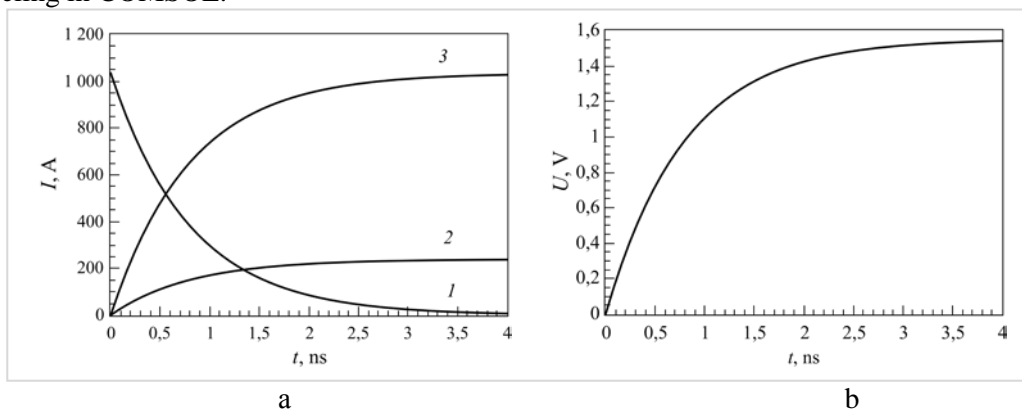


Figure 2. a) 1 – capacitive current flowing through sample I_{Scap} , A; 2 – conduction current (leakage current) of sample $I_{SR} \cdot 10^5$, A; 3- current through graphite matrix I_{GR} , A; b) voltage U_s , V on the sample.

As Figure 2 shows the conduction current magnitude passing through sample I_{SR} is much less than the magnitude of the current flowing through the graphite matrix I_{GR} ($I_{SR} / I_{GR} \sim 1 \cdot 10^{-6}$). The heating of the sample due to its own conductivity is not a chief source of thermal energy. At the moment of pulsing capacitive current I_{Scap} can reach peak output current of the pulsed source. In fact, the current curve of pulsed source cannot be instantly converted to maximum value because of the presence of inductivity in the circuit of the feeding transformer of SPS installation [9]. Maximum magnitude I_{Scap} will have less value. The flow of capacitive current is conditioned by the presence of polarized processes in the sample structure. Zirconium ions are displaced relatively the lattice sites. The distance of the resulted displacement is in direct proportion to the applied voltage. Thus the higher the voltage and the pulsed source current, the greater the displacement of zirconium ions. A similar stressed state in the lattice can reduce the amount of activation energy of the thermal diffusion process.

The operating voltage time on sample U_S amounts to about 4 ns. Considering the duration of the unit impulse of current, which is 25 ms, it is possible to state that the mechanical stress in the dioxide zirconium lattice is retained over the period of the whole pulse.

As it was mentioned earlier during analysis of the data from table 1 the energy of the electric field is not enough for formation of independent diffusion flow. The major role in emergence of mass transfer in the sintered sample belongs to thermal energy obtained from the graphite pressing-tool. Surface tension forces at points of contact of powder particles excite the processes of surface and inter-boundary diffusion. Owing to the presence of temperature gradient between the centre and periphery of the sample there is also a diffusion flow directed from the heated areas to cooler ones. This process is graphically demonstrated in fig.3, the arrows show the direction of thermal diffusion flow.

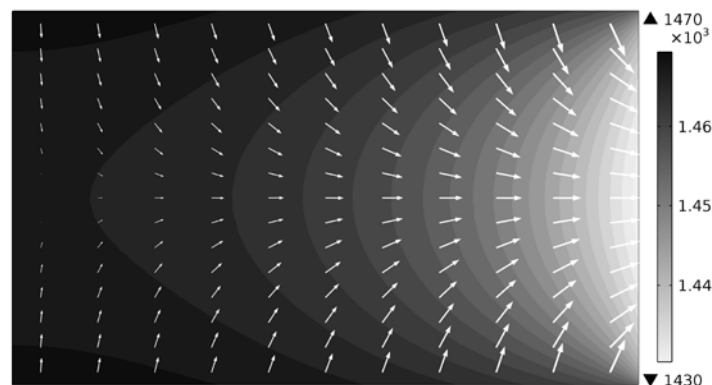


Figure 3. Thermal field in two-dimensional axisymmetric sample model, °C.

Since the axial pressure is applied to the sample in SPS process, plastic deformation [10] contributes to the mass transfer process as well. This phenomenon is the most vividly represented in sintering of malleable materials, for instance, metals.

4. Conclusions

A numerical modelling of thermal and electric field distribution in the graphite pressing-tool and in the sintered sample of stabilised zirconium dioxide in the process of sparkle plasma sintering has been conducted. By the results of calculation the primary mechanism of mass transfer at this sintering method has been determined. The reduction of sintering time at SPS is accounted for the large amount of the specific heat flow in the direction of sample surface arriving from the graphite pressing-tool. According to the data of the developed numerical model the average rate of uncontrolled sample heating made of stabilised zirconium dioxide with the diameter of 20 mm and the height of 6 mm with use of the pressing-tool, shown in Figure 1, amounts to ~ 900 °C/min. For comparison the heating rate

of the sintered material when using hot-pressing, which is also based on mutual use of Joule heat and axial pressure, does not exceed 80 °C/min.

The influence of the electric field on the sample structure results in appearance of polarized processes leading to displacement of zirconium ions from the lattice sites. Similar stressed state is capable of reducing the required amount of heat energy to start the diffusion process. In order to identify the signs of electromigration of zirconium ions under the influence of electric field an X-ray phase analysis (by means of 'Shimadzu XRD 6000' diffractometer) of the surface sample layers, sintered at temperature of 1300 °C, has been conducted. The relative density of the resulted ceramics was equal to 95.7 %, at the magnitude of the apparent density amounted to 6.04 g/cm³. The differences in the structure of the cathode and anode layers in comparison with the structure of the primary array have not been found. The tetragonal modification of zirconium dioxide amounted to 90 %, the rest 10 % belong to monoclinic modification.

The applied axial pressure at high temperatures of sintering can lead to plastic deformation of particles of the sintered powder body, which influences the reduction of time, required for complete removal of pores from ceramics.

5. Acknowledgments

This work was financially supported by the Russian President Grant (SP-1179.2015.1).

References

- [1] Annenkov Yu M et al. 2005 *Proceedings of Tomsk Polytechnic University* **7** (308) 39–43
- [2] Ivashutenko A S et al. 2008 *New refractory materials* **10** 35–42
- [3] Annenkov Yu M et al. 2006 *Radiation-thermal effects and processes in nonorganic materials: Proceedings of the Vth International scientific conference* vol 1 (Tomsk: TPU) p. 376–381
- [4] Matrenin S V, Slosman A I, Myachin Yu V 2005 *Proceed. of Tomsk Polyt. Univer.* **4** (308) 74–77
- [5] Batanov G M 2001 *JTP.* **7(71)** 119–123
- [6] Annenkov Yu M, Ivashutenko A S 2011 *Proceedings of universities Physics* **1** 37–39
- [7] Grasso S, Sakka Y, Maizza G Electric current activated/assisted sintering (ECAS): a review of patents 1906–2008 *Sci. Technol. Adv. Mater.* **5(10)** Article ID 053001
- [8] Molenat G et al. 2010 Temperature Control in Spark Plasma Sintering: An FEM Approach, *Journal of Metallurgy* Article ID 145431
- [9] Vanmeensel K et al. 2005 *Acta Materialia* **53** 4379–4388
- [10] Kornienko E, Smirnov A, Kuzmin V, 2015 *Applied Mechanics and Materials* **698** 405–410
- [11] Skeebe V, Pushnin V, Kornev D 2015 *Applied Mechanics and Materials* **788** 88–94
- [12] L I Shevtsova, M A Korchagin, A. Thommes, V I Mali, Anisimov A G, Nagavkin S Yu, 2014 *Advanced Materials Research* **1040** 772–777
- [13] Shevtsova L I, Mali V I, Bataev A A, Bataev I A, Terent'ev D S, Lozhkin V S 2013 *The 8 international forum on strategic technologies* **1** 187–189
- [14] Lazurenko D V, Mali V I, Anisimov A G, Yartsev P S, Lagereva D I, Shevtsova L I, 2014 *Advanced Materials Research* **1040** 800–804